ORIGINAL ARTICLE

Structural and proteomic repercussions of growth hormone receptor deficiency on the pituitary gland: Lessons from a translational pig model

Bachuki Shashikadze[1] | Sophie Franzmeier[2] | Isabel Hofmann[2] |
Martin Kraetzl[3,4] | Florian Flenkenthaler[1] | Andreas Blutke[2] |
Thomas Fröhlich[1] | Eckhard Wolf[1,3,4] | Arne Hinrichs[3,4]

[1]Laboratory for Functional Genome Analysis (LAFUGA), Gene Center, Ludwig-Maximilians-Universität München, Munich, Germany

[2]Institute of Veterinary Pathology at the Center for Clinical Veterinary Medicine, Ludwig-Maximilians-Universität München, Munich, Germany

[3]Chair for Molecular Animal Breeding and Biotechnology, Gene Center and Department of Veterinary Sciences, Ludwig-Maximilians-Universität München, Munich, Germany

[4]Center for Innovative Medical Models (CiMM), Ludwig-Maximilians-Universität München, Oberschleissheim, Germany

Correspondence
Arne Hinrichs, Chair for Molecular Animal Breeding and Biotechnology, Gene Center and Department of Veterinary Sciences, Ludwig-Maximilians-Universität München, Munich, Germany.
Email: a.hinrichs@gen.vetmed.uni-muenchen.de

Abstract

Growth hormone receptor deficiency (GHRD) results in low serum insulin-like growth factor 1 (IGF1) and high, but non-functional serum growth hormone (GH) levels in human Laron syndrome (LS) patients and animal models. This study investigated the quantitative histomorphological and molecular alterations associated with GHRD. Pituitary glands from 6 months old growth hormone receptor deficient (*GHR*-KO) and control pigs were analyzed using a quantitative histomorphological approach in paraffin (9 *GHR*-KO [5 males, 4 females] vs. 11 controls [5 males, 6 females]), ultra-thin sections tissue sections (3 male *GHR*-KO vs. 3 male controls) and label-free proteomics (4 *GHR*-KO vs. 4 control pigs [2 per sex]). *GHR*-KO pigs displayed reduced body weights (60% reduction in comparison to controls; $p < .0001$) and decreased pituitary volumes (54% reduction in comparison to controls; $p < .0001$). The volume proportion of the adenohypophysis did not differ in *GHR*-KO and control pituitaries (65% vs. 71%; $p = .0506$) and *GHR*-KO adenohypophyses displayed a reduced absolute volume but an unaltered volume density of somatotrophs in comparison to controls (21% vs. 18%; $p = .3164$). In *GHR*-KO pigs, somatotroph cells displayed a significantly reduced volume density of granules (23.5%) as compared to controls (67.7%; $p < .0001$). Holistic proteome analysis of adenohypophysis samples identified 4660 proteins, of which 592 were differentially abundant between the *GHR*-KO and control groups. In *GHR*-KO samples, the abundance of somatotropin precursor was decreased, whereas increased abundances of proteins involved in protein production, transport and endoplasmic reticulum (ER) stress were revealed. Increased protein production and secretion as well as significantly reduced proportion of GH-storing granules in somatotroph cells of the adenohypophysis without an increase in volume density of somatotroph cells in the adenohypophysis could explain elevated serum GH levels in *GHR*-KO pigs.

Bachuki Shashikadze, Sophie Franzmeier, Isabel Hofmann and Martin Kraetzl contributed equally to this work.

1 | INTRODUCTION

Growth hormone receptor deficiency (GHRD) is a rare autosomal recessive hereditary disorder caused by loss-of-function mutations of the *GHR* gene.[1] Affected patients (human Laron syndrome [LS])[2] as well as murine (the *Ghr*-KO mouse)[3] and porcine animal models (the *GHR*-KO pig)[4] display constantly elevated but non-functional levels of growth hormone (GH). The lack of GHR-mediated hepatic insulin-like growth factor 1 (IGF1) production leads to low circulating levels of IGF1 and a disturbed feedback regulation of pituitary GH release, causing constantly high GH levels in serum. The phenotypic consequences include inter alia postnatal growth retardation[2,4,5] and an increased accumulation of body fat[5–7] due the lack of lipolytic GH action.[8] Another consequence of GHRD is increased insulin sensitivity,[5–7] potentially associated with the lack of GH antagonism on insulin.[9]

While a correlation between low serum GH levels and reduced pituitary size has been observed in GH deficiency,[10] an enlargement of pituitary glands was not verified in LS patients using magnetic resonance imaging (MRI).[11] In contrast, when corrected for body weight, *Ghr*-KO mouse pituitaries were relatively enlarged and revealed an increased amount and proportion of GH producing somatotroph cells in the adenohypophysis.[12] Aim of the present study was to investigate the effects of a disturbed GH-IGF1 axis on structural and molecular characteristics of the pituitary gland in a large animal model for GHRD – the *GHR*-KO pig. We employed mass spectrometry-based label-free proteomics to reveal molecular changes and associated biological pathways in *GHR*-KO adenohypophysis. To complement molecular findings, further quantitative morphological analyses of the cellular composition of the adenohypophysis and the ultrastructure of somatotroph cells were performed. Specifically, the absolute volumes and volume proportions of the pituitary compartments, of the somatotroph cells in the adenohypophysis, and of the GH secretory granules in the somatotroph cells were determined, using unbiased quantitative-stereological analysis techniques.[13]

2 | MATERIALS AND METHODS

2.1 | Generation of pituitary gland tissue samples

All animal procedures were approved by the responsible animal welfare authority (Regierung von Oberbayern; permission 55.21-54-2532-70-12) and performed according to the German Animal Welfare Act and Directive 2010/63/EU for the protection of animals used for scientific purposes.

The present study examined pituitary glands (PG) from nine *GHR*-KO pigs (5 males and 4 females; age = 6 months) and 11 age-matched non-transgenic control littermates (5 males and 6 females) which were obtained in a previous study.[4] Pituitary glands were extracted as described previously[14] and weighed to the nearest milligram. The total volume of the PG ($V_{(PG)}$) was determined from its weight ($m_{(PG)}$) and its specific weight ($\gamma_{(PG)} = 0.89$ g/cm^3) as $V_{(PG)} = m_{(PG)}/\gamma_{(PG)}$.[13,15] Body weight and brain weight of the animals were also assessed in the same previous study.[4]

For holistic proteome analysis, a sample of approximately 1 mm^3 was excised from the adenohypophysis of four *GHR*-KO and four control animals (2 males and 2 females each) and immediately frozen on dry ice. The remaining pituitary gland was processed as described previously.[13–16] After fixation of the tissue in neutrally buffered 4% formaldehyde solution for 24 h at room temperature, the pituitary gland was exhaustively sliced into approximately 1 mm thick, parallel slabs.

For electron microscopy, each three tissue specimen of approximately 1 mm^3 were excised from the adenohypophysis (pars distalis) of three male *GHR*-KO and three male WT control animals, using a systematic random sampling approach.[13] These tissue samples were postfixed in 6.25% glutaraldehyde in Sorensen's phosphate buffer (Serva, USA) for 6 h and subsequently embedded in epoxy resin (Epon, aka glycidyl ether 100; methyl nadic anhydride; 2,4,6-tris [dimethylaminomethyl]phenol; 2-dodecyl succinic acid anhydride [Serva, USA]) in random orientation.[13] Subsequently, ultrathin tissue sections of approximately 70 nm were prepared and mounted on 1% formvar coated 200 mesh nickel grids (Veco, Neatherlands). Next, sections were treated with sodium metaperiodate (Merck, Germany) for 10 min and washed with deionized distilled H$_2$O (ddH$_2$O) for another 5 min. Consecutively, sections were incubated with 1% bovine serum albumin (BSA: Sigma Aldrich, USA) in ddH$_2$O solution for 5 min, 0.1 M phosphate-buffered saline (PBS) glycine buffer for 10 min and photo-tonic bandgap (PBG) buffer containing 0.2 g gelatin (Merck, Germany) and 0.5 g BSA three times for 2 min. Blocking was performed with normal donkey serum (Aurion, Netherlands) diluted 1:10 in PBS for 30 min. For unambiguous identification of somatotroph cells with GH-containing hormone granules and differentiation from other pituitary cell types, immuno-gold electron microscopy was used, as described previously.[17] For this, ultrathin sections were incubated with goat anti-GH antibody (R&D Systems, USA, 1:200 in PBS) at 4°C over night in a humid container. After washing with PBG six times for 2 min, sections were incubated with a 10-nm immuno-gold conjugated donkey anti-goat IgG antibody (Science Service GmbH, Germany, 1:50 in PBS) for 1 h at room temperature. Labeled sections were then washed with PBG, 0.1 M glycine-PBS and ultimately with ddH$_2$O. Finally, the slides were contrasted with 2% uranyl acetate (Science Service GmbH, Germany) and 3% lead citrate (Ultrostain II Leica, Germany) according to standard protocols. The sections were examined using and EM10 transmission electron microscope (Zeiss, Germany) at different magnifications.

For qualitative and quantitative histomorphological analyses, the remaining formalin-fixed pituitary gland tissue slabs were embedded in paraffin, while maintaining the orientation of their section surfaces. Sections of approximately 4 μm thickness were stained with hematoxylin and eosin (HE), and subjected to immunohistological detection of growth hormone (GH) using a specific polyclonal goat anti-rat GH antibody (#AF1566 R&D Systems, USA; 1:3000) and biotinylated rabbit anti-goat IgG solution (DAako, USA; 1:100), diaminobenzidine as chromogen and hemalum as nuclear counterstain, as previously described in detail.[13]

2.2 | Quantitative morphological analyses

2.2.1 | Determination of the volume of the adenohypophysis (AH) and the total volume of somatotrophs (SOM) in the AH

Volume densities ($V_{V(X/Y)}$) were estimated based on area densities using the principle of Delesse.[18,19] According to this principle, the volume density of a target structure $V_{(X)}$ in a reference compartment $V_{(Y)}$ is equal to the quotient of their respective cumulative section areas ($\sum A_{(X)}/\sum A_{(Y)}$). The so-called point counting method allows a simple determination of the area density ($A_{A(X/Y)}$) by calculating the quotient of the total number of points hitting section profiles of the target structure ($\sum Pt_{(X)}$) and the total number of points hitting the reference compartment ($\sum Pt_{(Y)}$) in the same sections.[20,21] The points can be represented by crosses to establish uniform rules regarding the "hitting" or "not hitting" of a point (Table S1).

The volume density of the adenohypophysis (AH) in the pituitary gland (PG) ($V_{V(AH/PG)}$) and the other pituitary compartments was determined as the fraction of the section areas of the AH (i.e., target structure) and the total section profile area of PG tissue (i.e., reference compartment) in HE stained paraffin sections of the PG (11 control and 9 GHR-KO) at 12.5× microscopic magnification based on the point density of the AH in the PG ($Pt_{Pt(AH/PG)}$) as described above and previously.[13] On the average, 750 ± 77 for the adenohypophysis, 665 ± 73 for the pars intermedia and 2260 ± 151 points were counted per case for the neurohypophysis (mean ± SE). The volume density of somatotroph cells in the AH ($V_{V(SOM/AH)}$) was analogously determined in immunohistological sections (11 control and 9 GHR-KO) in which somatotroph cells were identified by detection of GH, at 200× microscopic magnification, as the quotient of the total number of points hitting GH-positive cell section profiles ($\sum Pt_{(SOM)}$) and total number of points hitting AH-tissue section area ($\sum Pt_{(AH)}$) per case. On the average, 3326 ± 74 points were counted per case. The total volume of the AH ($V_{(AH, PG)}$) and the other compartments was then calculated as the product of $V_{(PG)}$ and $V_{V(AH/PG)}$ and the total volume of somatotrophs in the adenohypophysis ($V_{(SOM, AH)}$), respectively, as the product of $V_{V(SOM/AH)}$ and $V_{(AH, PG)}$ (Table S1).

2.2.2 | Determination of the volume of growth hormone granules in somatotroph cells by unbiased quantitative stereology

To estimate the volume density of GH containing granules (GH-GRAN) in somatotroph cells of the adenohypophysis ($V_{V(GH-GRAN/SOM)}$), ultrathin sections of two systematic uniform random (SUR) sampled locations of the adenohypophysis derived from three male control and three male GHR-KO pigs were analyzed by electron microscopy. In these sections, 29.8 ± 2.0 SUR sampled fields of view per case were photographed at 7000 x magnification. Within these areas, per case 51.0 ± 18.0 somatotroph cell section profiles were identified, based on their typical cellular morphological characteristics and detection of immuno-gold labeled GH-containing secretory granules.

$V_{V(GH-GRAN/SOM)}$ was determined, using the point counting method like described above and previously.[13] Per case, 2211.3 ± 287.0 points on somatotroph cells containing GH-containing granules per case were counted. The total volume of GH-granules in the somatotroph cells ($V_{(GH-GRAN,SOM)}$) was calculated by multiplication of $V_{V(GH-GRAN/SOM)}$ and the total volume of somatotroph cells in the adenohypophysis ($V_{(SOM, AH)}$) of the respective animal.

2.3 | Statistical analysis

Quantitative morphological data was statistically evaluated using a general linear models procedure (PROC GLM; SAS 8.2), taking the fixed effects of Group (GHR-KO, WT), Sex (male, female), and the interaction Group*Sex into account. Since none of the parameters was significantly affected by Sex and most were not affected by the interaction of Group*Sex (Table S2), least squares means (LSMs) and standard errors (SEs) of LSMs were calculated for the two groups and compared using student's t-tests. Correction for multiple testing was performed with the Bonferroni method using the ADJUST = BON statement. The ultrastructural measurements (GH granular) in three male control and three male GHR-KO pigs were compared using student t-tests using GraphPad Prism (GraphPad version 5.04).

2.4 | Sample preparation for proteome analysis

Frozen tissue samples from the adenohypophysis derived from four GHR-KO and four control animals (2 males and 2 females each) were transferred into precooled tubes and cryopulverized using a CP02 Automated Dry Pulverizer (Covaris, USA) according to the manufacturer's instructions. Next, ~10 mg of tissue powder was lysed in 8 M urea/50 mM ammonium bicarbonate by ultrasonication (18 cycles of 10 s pulse and 20 s pause) using a Sonopuls HD3200 (Bandelin, Germany). Protein content of lysates was quantified using a Pierce 660 nm Protein Assay (Thermo Fisher Scientific, USA). From each biological replicate, 20 μg of protein were further processed. Before

digestion, disulfide bonds were reduced (45 mM dithiothreitol/20 mM tris[2-carboxyethyl] phosphine, 30 min, 56°C) and cysteine residues were alkylated (100 mM iodoacetamide, 30 min, room temperature), followed by quenching of a residual iodoacetamide with dithiothreitol (90 mM, 15 min, room temperature). Proteins were digested with modified porcine trypsin (Promega, USA) for 16 h at 37°C (1:50 enzyme to protein ratio). Digested peptides were dried before analysis using a vacuum centrifuge.

2.5 | Nano-liquid chromatography (LC)–tandem mass spectrometry (MS/MS) analysis and bioinformatics

LC–MS/MS was performed on an UltiMate 3000 nano LC system online coupled to a Q-Exactive HF-X mass spectrometer via a nano-electrospray ion source (Thermo Fisher Scientific). Briefly, 1.5 μg of peptides were transferred to a PepMap 100 C18 trap column (100 μm × 2 cm, 5 μM particles, Thermo Fisher Scientific) at a flow rate of 5 μL/min mobile phase A (0.1% formic acid and 1% acetonitrile in water). Separation was performed on an analytical column (PepMap RSLC C18, 75 μm × 50 cm, 2 μm particles, Thermo Fisher Scientific) at 250 nL/min flow rate with a 160-min gradient of 3%–25% of solvent B, followed by a 10-min raise to 40% and 5-min raise to 85%. Solvent A was 0.1% formic acid in water and solvent B was 0.1% FA in acetonitrile. For mass spectrometry data acquisition cycles of one full scan and 15 data-dependent MS/MS scans were used. Raw files were processed with MaxQuant (version 1.6.7.0)[22] using its built-in search engine Andromeda[23] and the NCBI RefSeq Sus scrofa database (downloaded in April 2020) alongside the MaxQuant contaminants fasta file. Protein intensities were normalized with the MaxLFQ label-free normalization approach.[24] All statistical and bioinformatic analyses were done using Perseus (version 1.6.7.0)[25] or the R framework.[26] Proteins detected in at least 70% of all replicates in at least one condition were kept for quantitative analysis. To handle missing values, data imputation from a normal distribution was performed using the Perseus default parameters (width – 0.3 and down-shift – 1.8). A volcano plot was generated with Perseus using two-tailed Student's *t*-test statistics and permutation-based FDR cutoff of 0.05, together with an s0-parameter of 0.1 to additionally consider fold changes.[27] When appropriate, comparisons between multiple conditions were performed using a two-way analysis of variance (ANOVA). Resulting *p*-values were corrected for multiple hypothesis testing using the Benjamini-Hochberg (BH) procedure. Proteins with a significant two-way ANOVA interaction effect (adjusted *p*-value <.05) were followed by a Tukey's HSD post hoc test. For unsupervised cluster analysis, principal component analysis (PCA) (prcomp() function with default parameters in R) and hierarchical clustering (ComplexHeatmap R package[28]) was applied. Overrepresentation analysis, based on significantly changed proteins was performed using WebGestalt[29] and the functional category "GO Biological Process

nonRedundant". False discovery rate was controlled using BH procedure. All data visualization was performed in R.[26]

3 | RESULTS

3.1 | *GHR*-KO pigs display significantly reduced body weights, pituitary-, adenohypophyseal-, and total somatotroph-volumes

GHR-KO pigs investigated in this study showed a significant, 60% reduction in body weight (Figure 1A), as compared to controls (38.5 ± 3.6 kg vs. 97.5 ± 3.3 kg; $p < .0001$). Correspondingly, the absolute weights and volumes of the pituitary glands ($V_{(PG)}$) of *GHR*-KO pigs were also significantly reduced by 54% (126.6 ± 8.4 mg/115.1 ± 7.6 mm^3 in *GHR*-KO vs. 273.8 ± 7.6 mg / 248.9 ± 6.9 mm^3 in controls; $p < .0001$) (Figure 1B). When corrected for body weight, the relative weight of *GHR*-KO pituitary glands was only 1.15-times larger than in control pigs ($p = .0367$) (Figure 1C). The absolute brain weight was only reduced by approximately 15% in *GHR*-KO pigs (83.4 ± 2.6 g in *GHR*-KO vs. 95.6 ± 2.3 g in controls; $p = .0017$) (Table 1). Accordingly, relative brain weight of *GHR*-KO animals was more than doubled (by factor 2.2 of control animal's values; $p < .0001$; see Table 1). The reduction in pituitary gland weight and volume was not in proportion to brain weight reduction (see Table 1).

While the volume proportion of the adenohypophysis (i.e., pars distalis) in the pituitary gland ($V_{V(AH/PG)}$) was not significantly different in *GHR*-KO and control pigs (0.65 ± 0.02 in *GHR*-KO vs. 0.7 ± 0.02 in controls; $p = .0506$; Figure 1D), the absolute volume of the adenohypophysis ($V_{(AH, PG)}$) in *GHR*-KO pigs was also significantly lower than in controls (75.4 ± 6.8 mm^3 in *GHR*-KO vs. 176.1 ± 6.2 mm^3 in controls; $p < .0001$; Figure 1E). While the reduction of volumes of pituitary compartments appeared in correspondence to the reduction in body weight, the neurohypophysis (i.e., pars nervosa) in the pituitary gland was less affected by growth retardation, as the volume proportion of the neurohypophysis in the pituitary gland ($V_{V(NH/PG)}$) appeared increased (0.27 ± 0.02 in *GHR*-KO vs. 0.22 ± 0.01 in controls; $p = .039$) as well as the relative volume (rel. $V_{(NH, PG)}$; 0.81 ± 0.05 mm^3 per kg BW in *GHR*-KO vs. 0.57 ± 0.05 mm^3 per kg BW in controls; $p = .0026$) when corrected for body weight (see Table 1).

The volume proportion of somatotroph cells in the adenohypophysis ($V_{V(SOM/AH)}$) was also not significantly different in *GHR*-KO and control pigs (0.21 ± 0.02 in *GHR*-KO vs. 0.18 ± 0.02 in controls; $p = .3164$; Figure 1F and 2A), while the total volume of somatotroph cells in the adenohypophysis ($V_{(SOM, AH)}$) of *GHR*-KO pigs was correspondingly significantly lower as compared to controls (15.9 ± 3.2 mm^3 in *GHR*-KO vs. 32.3 ± 2.9 mm^3 in controls; $p = .0016$; Figure 1G).

None of the investigated parameters revealed an effect for sex (see Table S2). Solely for the absolute and relative volume of the pars intermedia ($V_{(pars\ intermedia,\ PG)}$ $p = .0464$; rel. $V_{(pars\ intermedia,\ PG)}$ $p = .0192$) and the volume proportion of the pars intermedia in the
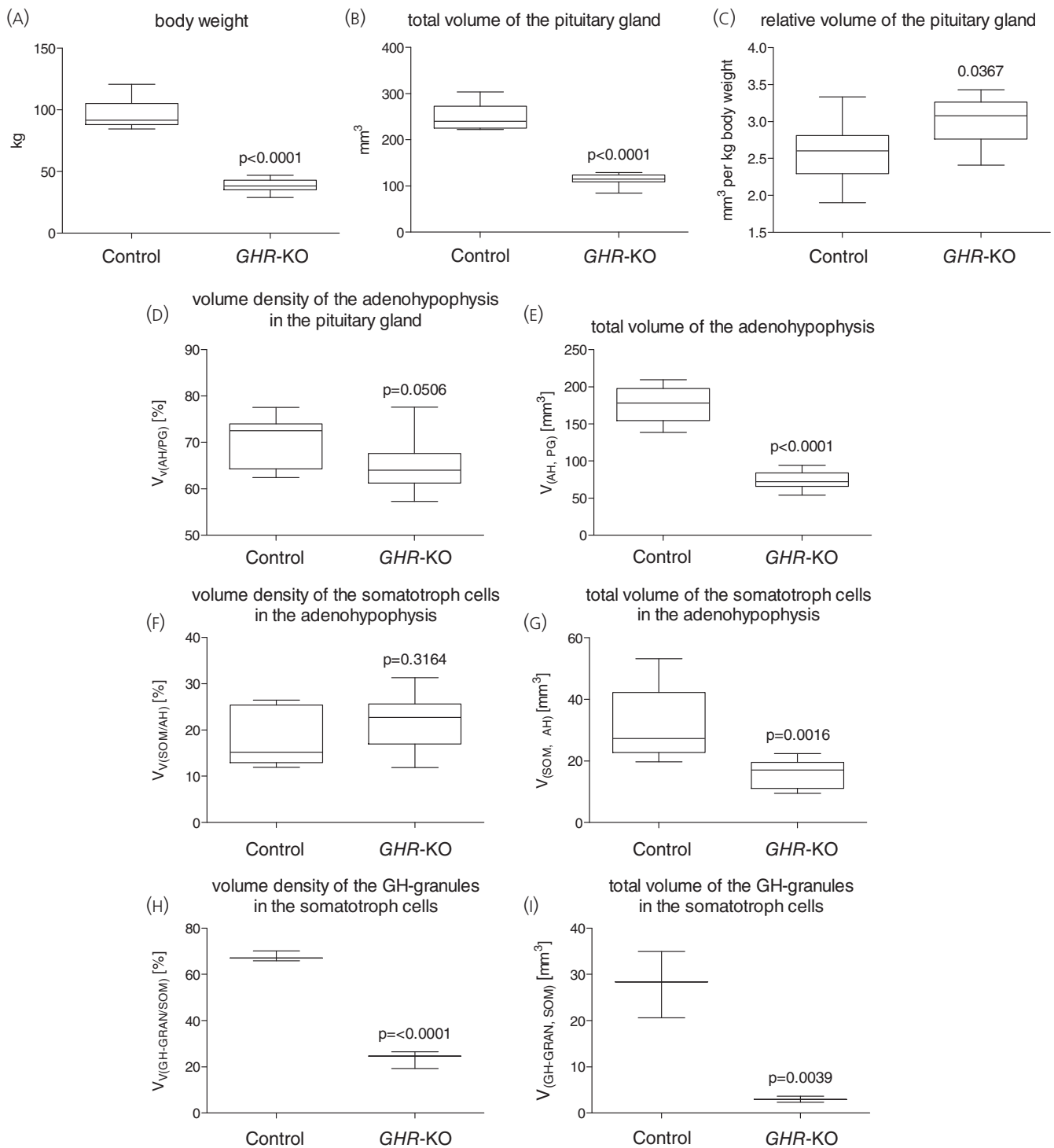
FIGURE 1 (A, C) GHR-KO pigs (9 GHR-KO [5 males; 4 females] vs. 11 control pigs [5 males; 6 females]) display significantly reduced body weights (A) and pituitary gland (PG) volumes (B), as compared to control pigs. The volume of GHR-KO pituitary glands appears just slightly increased when corrected for body weight (C). (D–I) Quantitative morphological analysis of the pituitary gland and somatotroph cells. The volume density of the adenohypophysis (AH) in the pituitary gland (D) and the volume density of the somatotroph cells (SOM) in the AH (F) do not significantly differ between control- and GHR-KO pigs. Corresponding to the reduced volume of the PG, the absolute volumes of the AH- and the somatotroph cells (E, G) are significantly reduced in GHR-KO pigs. The volume density (H), as well as the absolute volume of growth hormone-containing secretory granules in somatotroph cells (I), however, is significantly reduced in GHR-KO pigs (3 male GHR-KO vs. 3 male control pigs; compare to Figure 2B). The box plots show medians, 25th and 75th percentiles (box), and extremes (whiskers).

TABLE 1 Growth parameters and quantitative stereological data of control and *GHR*-KO pigs.

Parameter	Control	*GHR*-KO	*p*-value
Body weight (BW) (kg)	97.5 ± 3.3	38.5 ± 3.6	<.0001
Brain weight (g)	95.6 ± 2.3	83.4 ± 2.6	.0028
Rel. brain weight (% of BW)	0.1 ± 0.008	0.2 ± 0.009	<.0001
weight of pituitary glands (PG) (mg)	273.8 ± 7.6	126.6 ± 8.4	<.0001
Rel. weight of pituitary glands (% of BW x 10^{-3})	0.28 ± 0.014	0.33 ± 0.019	.0367
Rel. weight of pituitary glands (% of brain weight)	0.29 ± 0.011	0.15 ± 0.012	<.0001
$V_{(PG)}$ (mm^3)	248.9 ± 6.9	115.1 ± 7.6	<.0001
Rel. $V_{(PG)}$ (mm^3 per kg BW)	2.6 ± 0.1	3.0 ± 0.1	.0367
rel. $V_{(PG)}$ (mm^3 per g brain weight)	2.6 ± 0.1	1.4 ± 0.1	<.0001
$V_{V(AH/PG)}$	0.71 ± 0.02	0.65 ± 0.02	.0506
$V_{V(pars\ intermedia/PG)}$	0.07 ± 0.005	0.06 ± 0.006	.1814
$V_{V(NH/PG)}$	0.22 ± 0.01	0.27 ± 0.02	.039
$V_{(AH,\ PG)}$ (mm^3)	176.1 ± 6.2	75.4 ± 6.8	<.0001
$V_{(pars\ intermedia,\ PG)}$ (mm^3)	18.2 ± 1.2	7.2 ± 1.4	<.0001
$V_{(NH,\ PG)}$ (mm^3)	55.0 ± 3.1	31.0 ± 3.4	<.0001
Rel. $V_{(AH,\ PG)}$ (mm^3 per kg BW)	1.8 ± 0.1	2.0 ± 0.1	.4395
Rel. $V_{(pars\ intermedia,\ PG)}$ (mm^3 per kg BW)	0.19 ± 0.02	0.18 ± 0.02	.9938
Rel. $V_{(NH,\ PG)}$ (mm^3 per kg BW)	0.57 ± 0.05	0.81 ± 0.05	.0026
rel. $V_{(AH,\ PG)}$ (mm^3 per g brain weight)	1.9 ± 0.08	0.9 ± 0.09	<.0001
Rel. $V_{(pars\ intermedia,\ PG)}$ (mm^3 per g brain weight)	0.19 ± 0.02	0.09 ± 0.02	.0002
Rel. $V_{(NH,\ PG)}$ (mm^3 per g brain weight)	0.58 ± 0.03	0.37 ± 0.04	.0009
$V_{V(SOM/AH)}$	0.18 ± 0.02	0.21 ± 0.02	.3164
$V_{(SOM,\ AH)}$ (mm^3)	32.3 ± 2.9	15.9 ± 3.2	.0016
Rel. $V_{(SOM,\ AH)}$ (mm^3 per kg BW)	0.34 ± 0.04	0.4 ± 0.04	.2464
Rel. $V_{(SOM,\ AH)}$ (mm^3 per g brain weight)	0.35 ± 0.03	0.19 ± 0.04	.0079
$V_{V(GH-GRAN/SOM)}$	0.68 ± 0.02	0.24 ± 0.02	<.0001
$V_{(GH-GRAN,\ SOM)}$ (mm^3)	27.97 ± 4.16	2.997 ± 0.38	.0039

Note: Body weight, brain weight and pituitary data was assessed from 11 control (5 males; 6 females) and nine *GHR*-KO pigs (5 males; 4 females) in a previous study (Hinrichs et al., 2018) and were statistically evaluated using a general linear models procedure (PROC GLM; SAS 8.2), taking the fixed effects of Group (*GHR*-KO, WT), Sex (male, female), and the interaction Group*Sex into account. Since none of the parameters were significantly affected by Sex and most were not affected by the interaction of Group*Sex (Table S2), least squares means (LSMs) and standard errors (SEs) of LSMs were calculated for the two groups and compared using student *t*-tests. Correction for multiple testing was performed with the Bonferroni method using the ADJUST = BON statement. The ultrastructural measurements (GH granula) in three male control and three male *GHR*-KO pigs were compared using student *t*-tests using GraphPad Prism (GraphPad Version 5.04).
Abbreviations: AH, adenohypophysis; BW, body weight; GH-GRAN, GH-containing secretory granules; NH, neurohypophysis; PG, pituitary gland; Rel., relative; SOM, somatotroph cells.

pituitary gland showed an effect for the interaction of group*sex ($V_{V(pars\ intermedia/PG)}$ *p* = .0321) (see Table S2).

3.2 | Somatotroph cells in *GHR*-KO pigs display significantly reduced relative and absolute volumes of secretory granules

Ultrastructural quantitative-morphological analysis of somatotroph cells revealed a significant reduction of the relative volume of

secretory granules in *GHR*-KO pigs (Figures 1H and 2B). The volume density of secretory granules in somatotroph cells in the adenohypophysis ($V_{V(GH-GRAN/SOM)}$) in *GHR*-KO pigs (23.5 ± 2.2%) was reduced by 65% (*p* < .0001), as compared to control pigs (67.7 ± 2.2%). Correspondingly, the total volume of GH-containing secretory granules in somatotroph cells of *GHR*-KO pigs ($V_{(GH-GRAN,\ SOM)}$) was also significantly reduced (3.0 ± 0.4 mm^3 in *GHR*-KO vs. 28.0 ± 4.2 mm^3 in controls; *p* = .0039) (Figure 1I). Occasionally, mild dilation of the ER was observed in somatotroph cell section profiles of *GHR*-KO pigs. However, this observation was not further

FIGURE 2 (A) Immunohistological detection of growth hormone (brown color) in somatotroph cells in the adenohypophysis of Control- and *GHR*-KO pigs. In *GHR*-KO pigs, somatotroph cell section profiles display a granular staining pattern with a slightly weaker staining intensity as compared to control pigs. Formalin-fixed, paraffin-embedded tissue sections. Bars = 50 μm and 25 μm in insets. (B) Somatotroph cell ultrastructure. Somatotrophs (som) of *GHR*-KO pigs apparently display fewer hormone granule section profiles than controls. Transmission electron microscopy. Arrows indicate immuno-gold labeled GH-containing secretory granules. Bars = 2.5 μm and 500 nm in insets.
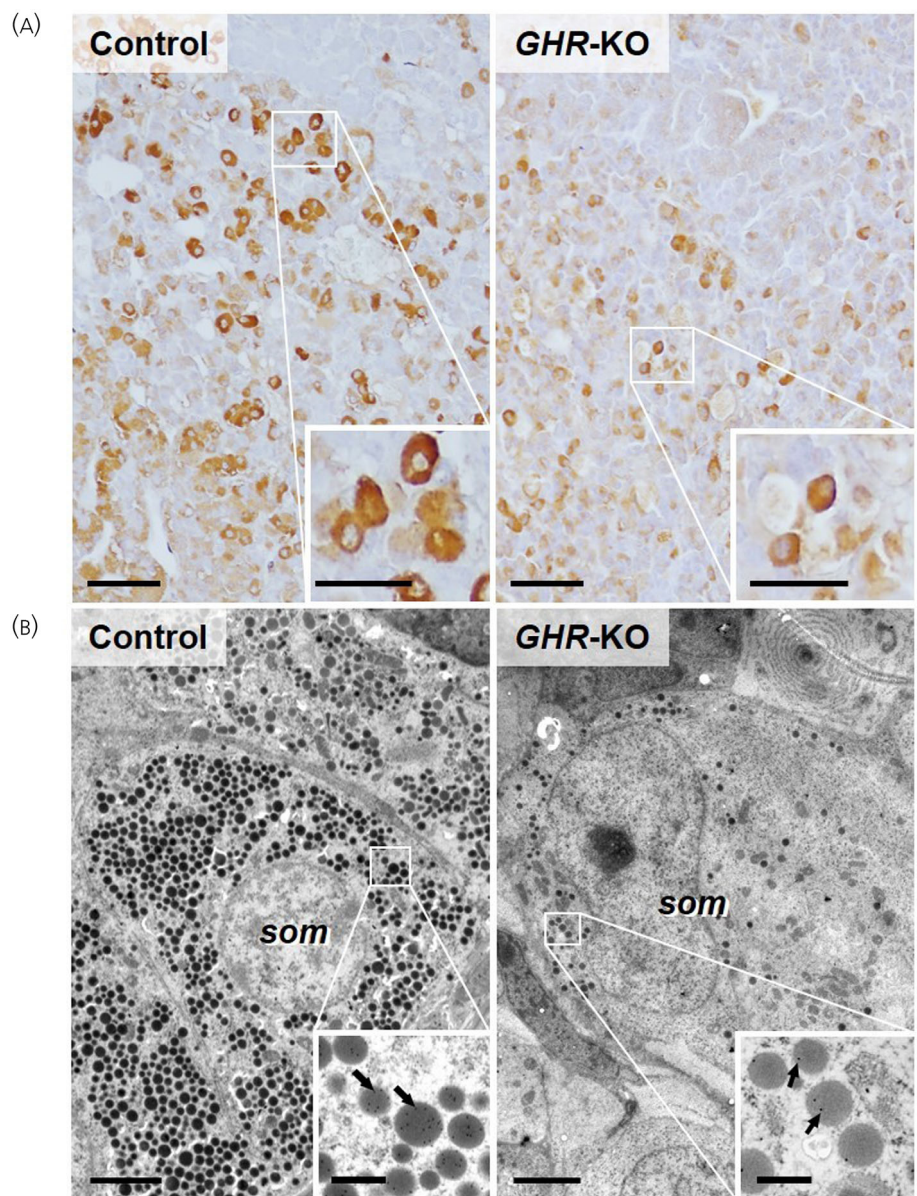

quantitatively analyzed on a morphological level due to occurrence in only a minor proportion of the examined somatotroph cell cross section profiles.

3.3 | GHRD leads to major alterations of the adenohypophysis proteome profile

In total, 44,860 peptides were identified which could be assigned to 4660 protein groups at an FDR <0.01 (Table S3). The dataset has been submitted to the ProteomeXchange Consortium via the PRIDE[30] partner repository (PXD035833). Unsupervised hierarchical clustering (Figure 3A) and principal component analysis (Figure 3B) of the proteome data revealed a clear genotype-dependent separation of the samples. A two-sided *t*-test with a permutation-based FDR approach revealed 369 significantly (FDR <0.05) more abundant proteins and 223 less abundant proteins in *GHR*-KO versus control samples (Figure 3C, Table S3). Among the proteins with the highest abundance increase (indicated as log2-fold change [l2fc]) in *GHR*-KO adenohypophysis were glycoprotein hormones alpha chain precursor (CGA; l2fc 5.3), followed by argininosuccinate synthase (ASS1, l2fc 3.9). Likewise, other proteins involved in amino acid metabolism, such as pyrroline-5-carboxylate reductase 1, mitochondrial isoform X3 (PYCR1, l2fc 2.7), and CAD protein (CAD, l2fc 2.6) were elevated. Furthermore, ribosomal proteins, for example, 40S ribosomal protein S26 (RPS26, l2fc 2.7), 60S ribosomal protein L15 isoform X1 (RPL15, l2fc 2.7), and 60S ribosomal protein L36 (RPL36; l2fc 2.2) were among the most significantly elevated proteins. The set of proteins most decreased in abundance in *GHR*-KO adenohypophysis contained among other proteins involved in retinol metabolism, such as retinoic
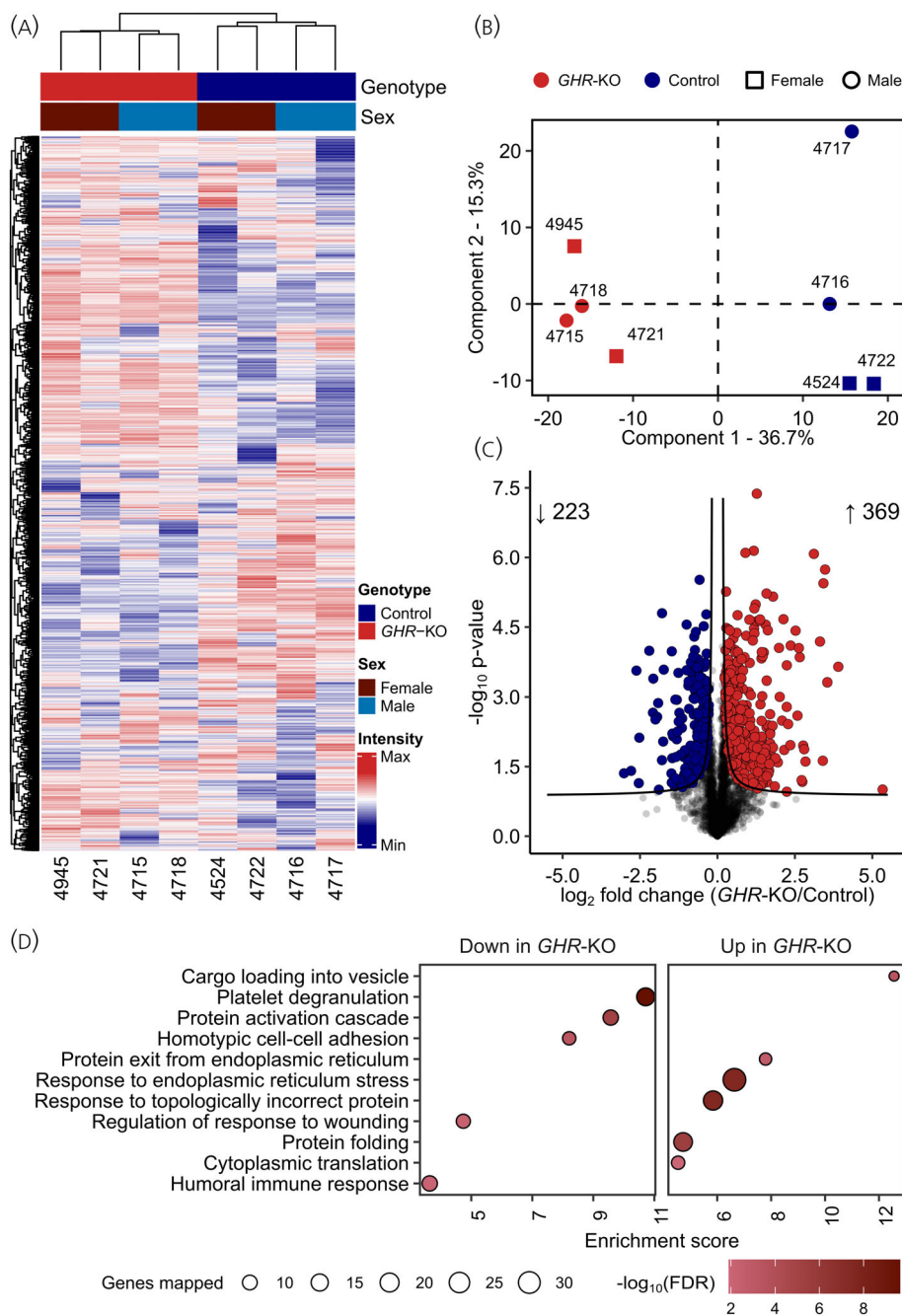
FIGURE 3 Quantitative proteome analysis of adenohypophysis from _GHR_-KO and control pigs. (A) Label-free quantitation (LFQ) intensity values of adenohypophysis proteomes of each sample (_GHR_-KO: $n = 2$ female, $n = 2$ male; control, $n = 2$ female, $n = 2$ male) were grouped by unsupervised hierarchical clustering and visualized as a heatmap. The color code indicates z-score normalized abundance values. (B) Principal component analysis indicates genotype (_GHR_-KO vs. control) as the strongest contributor to the intersample variance of the adenohypophysis proteome. The shape of each spot corresponds to the sex, and the color to the genotype. (C) Volcano plot visualizes the protein abundance change between conditions (_GHR_-KO/control). Proteins significantly altered in abundance (FDR < 0.05) are colored in red and blue for increased and decreased abundance, respectively. Black curves represent the permutation-based false discovery rate (FDR) significance cutoff. (D) Overrepresentation analysis of adenohypophysis proteins less abundant in _GHR_-KO (left column) and more abundant in _GHR_-KO (right column). Size of each bubble indicates the corresponding number of differentially abundant proteins (referred to as genes mapped in the figure) and color the significance of enrichment. Enrichment score is magnitude of overrepresentation. Multiple testing correction was performed using BH method.

acid receptor responder protein 1 (RARRES1; l2fc −3.0) and retinol-binding protein 4 isoform X1 (RBP4; l2fc −2.0). Furthermore, somatotropin precursor (GH1; l2fc −1.8) was decreased in abundance.

Overrepresentation analysis using the significantly changed proteins revealed 36 gene sets significantly enriched in _GHR_-KO pig's adenohypophysis and 45 gene sets enriched in control pig's adenohypophysis (FDR <0.05) (Table S5). Inter alia, gene sets such as response to endoplasmic reticulum stress, cargo loading into vesicle, protein exit from endoplasmic reticulum, response to topologically incorrect protein, protein folding, and cytoplasmic translation were

overrepresented among the proteins increased in abundance in _GHR_-KO pig's adenohypophysis (Figure 4), whereas gene sets such as platelet degranulation, protein activation cascade, homotypic cell–cell adhesion, regulation of response to wounding, and humoral immune response were overrepresented among the proteins increased in abundance in control pig's adenohypophysis (Figure 3D). In addition, two-way ANOVA revealed five proteins that were differently abundant with an effect for sex and the abundance of only four proteins were significantly influenced by the interaction of group x sex (Table S6).
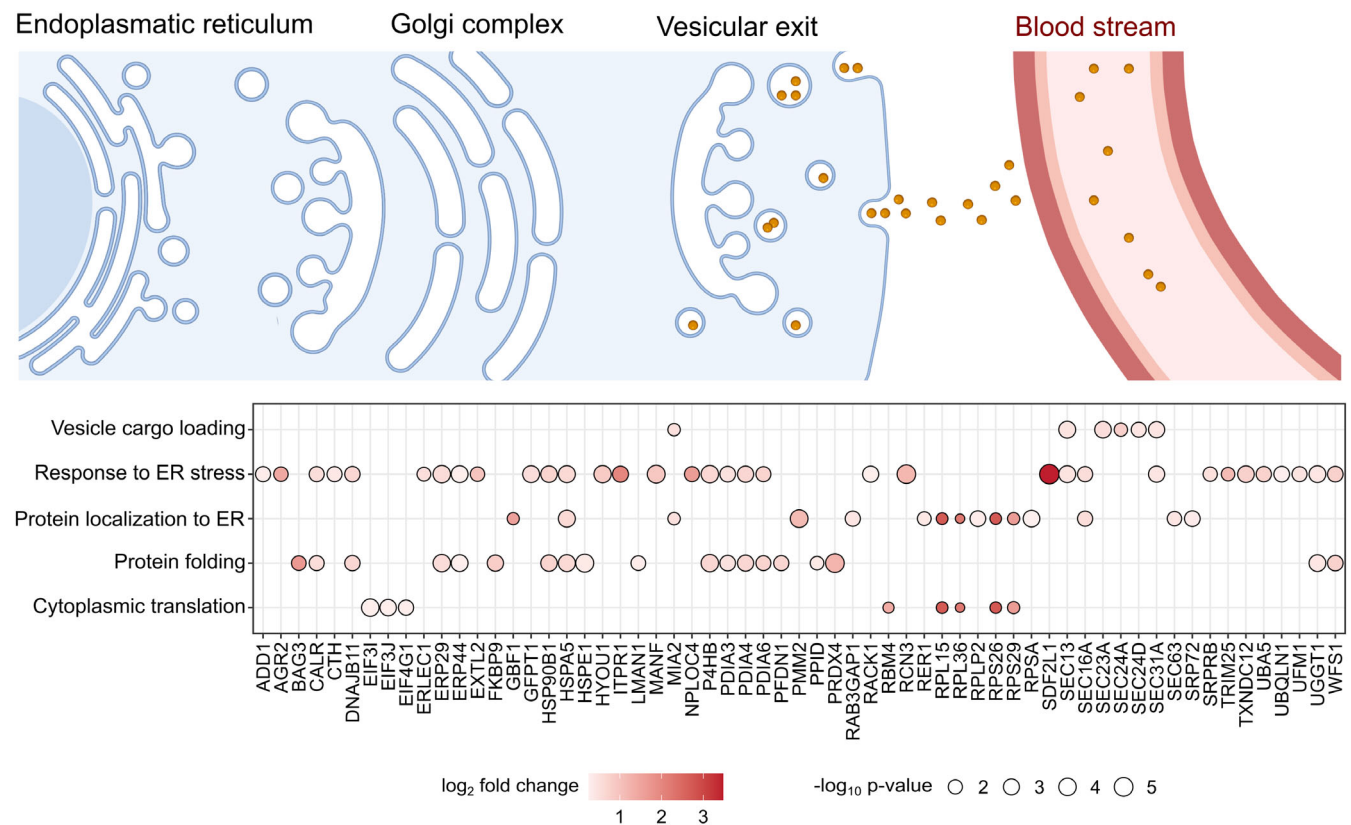
FIGURE 4 Increased protein production and secretion in *GHR*-KO adenohypophyses. Bubble plot of differentially abundant proteins that are involved in the following processes: vesicle cargo loading, response to ER stress, protein localization to ER, protein folding and cytoplasmic translation. The color of the bubble corresponds to the log2-fold change of protein (red downregulation, blue upregulation) and the size of the bubble indicates the significance of the protein change (bottom). ER, endoplasmic reticulum. The top part of this figure was generated using BioRender.

4 | DISCUSSION

The aim of this study was to investigate the histomorphological and molecular alterations of the adenohypophysis in the pathophysiological condition of GHRD.

Under physiological conditions (functional GHR), GH is secreted in a pulsatile manner from secretory granules storing GH (reviewed in[31]). In contrast, baseline serum GH levels are constantly elevated in GHRD and show higher peaks[32] due to the lack of IGF1 mediated negative feedback regulation. In association with high serum GH levels, a study in *Ghr*-KO mice pituitaries indicated an increased proportion of GH producing somatotroph cells.[12] Other adenohypophyseal cell populations (lactotroph, corticotroph, tyrotroph and gonadotroph) remained with unaltered distribution and proportional reduction. Nevertheless, no pituitary hypertrophy was detected in human LS patients despite high levels of GH.[11] Porcine pituitaries show close similarities to human pituitaries regarding histological and stereological composition.[33] In humans, somatotroph cells make up about 50% of hormone-producing cells in the adenohypophysis,[34] which appears in line with observations in pigs[33] and also in mice,[35] with a dependency on age and genetic background. We recently confirmed that *GHR*-KO pigs resemble the hallmark for GHRD, which

are elevated GH and decreased IGF1 levels.[4] For an objective quantitative assessment of the effects of GHRD on relevant morphological characteristics of the porcine pituitary gland and somatotroph cells, established unbiased quantitative-stereological analyses were[13–16] applied, demonstrating that the volume proportions of the adenohypophysis in the pituitary gland, and of somatotroph cells in the adenohypophysis were not significantly altered in *GHR*-KO pigs. Interestingly, the volume density of GH-containing secretory granules in somatotroph cells of *GHR*-KO pigs was significantly reduced. This is in line with the 3.5-fold decreased abundance of somatotropin precursor (GH1) revealed by proteomic analysis. Together with their increased systemic GH-levels,[4] the reduced proportion of secretory granules in somatotroph cells of *GHR*-KO pigs could be interpreted as a consequence of a permanently increased release of GH due to a lack of feedback inhibition. An increased protein production is also indicated in proteomic data of *GHR*-KO pig adenohypophysis as several 40S (RPSA, RPS26, RPS29) and 60S ribosomal subunits (RPLP2, RPL15, RPL36) were increased in abundance, which are inter alia associated with the enriched gene sets "translational initiation", "cytoplasmic translation" and "protein localization to endoplasmic reticulum". Following an increased protein translation, several proteins located in the ribosome, such as disulfide

isomerases (inter alia ERP44, PDIA3, PDIA4, PDIA6) and chaperones (inter alia UGGT1, HSP90B1), associated with the enriched gene set "protein folding" showed an increase in abundance. For the transport from the ER to the Golgi complex, proteins are packed in COPII-coated vesicles. Their components are formed by protein transport proteins whose abundance was significantly increased in *GHR*-KO adenohypophysis (SEC13, SEC23A, SEC24A, SEC24D, SEC31A), which were related to the enriched gene set "cargo loading vesicle" and "protein exit from ER". The increased demand for peptide hormones requires an adaptation by expanding ER membranes and can increase the amount of unfolded proteins in cells, which can cause ER stress.[36] Accordingly, the most prominent proteins increased in *GHR*-KO adenohypophysis were related to "response to ER stress", followed by "response to topologically incorrect protein". Those pathways contained prominent proteins involved in ER-associated degradation (ERAD) of misfolded proteins, such as ERLEC1, HSP90B1, DNAJB11, UBQLN1, and chaperones (MANF, HYOU1, HSPA5).

In conclusion, proteomic analysis together with quantitative histomorphological analysis findings suggest increased production and release of GH, while the volume proportion of the adenohypophysis (i.e., pars distalis) in the pituitary gland and the volume proportion of somatotroph cells in the adenohypophysis remain unaffected. This might explain the observation of unaffected pituitary size in human LS patients.

In addition to GH from somatotroph cells, the anterior pituitary secrets glycoproteins derived from gonadotropic (follicle-stimulating and luteinizing hormone – FSH and LH) and thyrotrophic cells (thyroid-stimulating hormone [TSH]) formed as dimers from a shared alpha chain and a hormone-specific beta subunit.[37] Since the glycoprotein hormones alpha chain precursor (CGA) showed an increased abundance in *GHR*-KO adenohypophysis samples and disturbances in at least thyroid hormone levels are reported from mice,[38] future studies should aim to investigate glycoproteins in GHRD.

In contrast to the majority of other tissues and organs, development and growth of the brain appear to be largely independent of GH action, resulting in an increased brain weight to body weight-ratio in *GHR*-KO pigs[4] and *Ghr*-KO mice.[39] In contrast, giant transgenic mice overexpressing GH have a decreased relative brain weight.[40] A study by Asa et al.[12] inter alia assessed the weight of pituitary glands in *Ghr*-KO mice and observed that the reduction of pituitary weights was less than the reduction of overall body weight. In the present study, we showed that the pituitary compartments are differently affected by GHRD. While absolute volumes of all pituitary compartments were reduced, only the volumes of the adenohypophysis and pars intermedia were reduced in proportion to body weight, while the neurohypophysis was less affected. In contrast to the adenohypophysis and pars intermedia, which are derived from the ectoderm, the neurohypophysis is derived from the base of the diencephalon as a part of the neuroectoderm.[41] Therefore, the same (unclassified) mechanisms leading to the GH-independent growth of the brain, might possibly also affect the neurohypophysis.

5 | CONCLUSION

This study investigated histomorphological, ultrastructural and molecular alterations of the pituitary gland in a translational pig model for GHRD. Quantitative stereological analyses identified functionally relevant morphological alterations of somatotroph cells in the pituitary gland supporting the interpretation of alterations of the pituitary proteome profile and increased serum GH levels. The latter are neither associated with a relative enlargement of the adenohypophysis in *GHR*-KO pituitaries nor a significant increase in the volume density of somatotroph cells in the adenohypophysis. In fact, high serum GH levels appear to represent a consequence of increased protein production and secretion, leading to a depletion of GH-containing granules in somatotroph cells.

AUTHOR CONTRIBUTIONS

Bachuki Shashikadze: Formal analysis; investigation; methodology; writing – review and editing. **Sophie Franzmeier:** Formal analysis; investigation; methodology. **Isabel Hofmann:** Data curation; formal analysis; investigation; methodology; writing – review and editing. **Martin Kraetzl:** Data curation; formal analysis; investigation; methodology. **Florian Flenkenthaler:** Data curation; formal analysis; investigation; methodology. **Andreas Blutke:** Conceptualization; data curation; formal analysis; investigation; methodology; writing – review and editing. **Thomas Fröhlich:** Conceptualization; data curation; formal analysis; investigation; methodology; writing – review and editing. **Eckhard Wolf:** Writing – review and editing. **Arne Hinrichs:** Conceptualization; data curation; formal analysis; investigation; project administration; supervision; writing – original draft; writing – review and editing.

CONFLICT OF INTEREST STATEMENT

The authors have no conflicts of interest to disclose.
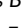
PEER REVIEW

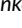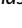The peer review history for this article is available at https://www.webofscience.com/api/gateway/wos/peer-review/10.1111/jne.13277.

DATA AVAILABILITY STATEMENT

The proteome dataset is available at ProteomeXchange (PXD035833). The code to reproduce the proteomics analyses and figures presented in this study can be found at: https://github.com/bshashikadze/GHR-KO-proteomics-2022.

ORCID

Bachuki Shashikadze (ID) https://orcid.org/0000-0003-4558-0785

Sophie Franzmeier (ID) https://orcid.org/0000-0002-1265-6790

Isabel Hofmann (ID) https://orcid.org/0000-0003-4019-9619

Martin Kraetzl (ID) https://orcid.org/0000-0002-8449-177X

Florian Flenkenthaler (ID) https://orcid.org/0000-0003-2964-9236

Andreas Blutke (ID) https://orcid.org/0000-0001-7824-2681

Thomas Fröhlich (ID) https://orcid.org/0000-0002-4709-3211

Eckhard Wolf (ID) https://orcid.org/0000-0002-0430-9510

Arne Hinrichs (ID) https://orcid.org/0000-0003-3022-5983

REFERENCES

1. Eshet R, Laron Z, Pertzelan A, Arnon R, Dintzman M. Defect of human growth hormone receptors in the liver of two patients with Laron-type dwarfism. *Isr J Med Sci*. 1984;20(1):8-11.

2. Laron Z. Laron syndrome (primary growth hormone resistance or insensitivity): the personal experience 1958-2003. *J Clin Endocrinol Metab*. 2004;89(3):1031-1044.

3. Zhou Y, Xu BC, Maheshwari HG, et al. A mammalian model for Laron syndrome produced by targeted disruption of the mouse growth hormone receptor/binding protein gene (the Laron mouse). *Proc Natl Acad Sci U S A*. 1997;94(24):13215-13220.

4. Hinrichs A, Kessler B, Kurome M, et al. Growth hormone receptor-deficient pigs resemble the pathophysiology of human Laron syndrome and reveal altered activation of signaling cascades in the liver. *Mol Metab*. 2018;11:113-128.

5. List EO, Sackmann-Sala L, Berryman DE, et al. Endocrine parameters and phenotypes of the growth hormone receptor gene disrupted (GHR−/−) mouse. *Endocr Rev*. 2011;32(3):356-386.

6. Guevara-Aguirre J, Rosenbloom AL, Balasubramanian P, et al. GH receptor deficiency in Ecuadorian adults is associated with obesity and enhanced insulin sensitivity. *J Clin Endocrinol Metabol*. 2015; 100(7):2589-2596.

7. Hinrichs A et al. Transient juvenile hypoglycemia in growth hormone receptor deficiency–mechanistic insights from Laron syndrome and tailored animal models. *Eur J Endocrinol*. 2021;185(2):R35-R47

8. Vijayakumar A, Novosyadlyy R, Wu YJ, Yakar S, LeRoith D. Biological effects of growth hormone on carbohydrate and lipid metabolism. *Growth Hormone IGF Res*. 2010;20(1):1-7.

9. Dominici FP, Turyn1 D. Growth hormone-induced alterations in the insulin-signaling system. *Exp Biol Med*. 2002;227(3):149-157.

10. Nagel BHP, Palmbach M, Petersen D, Ranke MB. Magnetic resonance images of 91 children with different causes of short stature: pituitary size reflects growth hormone secretion. *Eur J Pediatr*. 1997;156(10): 758-763.

11. Kornreich L, Horev G, Schwarz M, Karmazyn B, Laron Z. Pituitary size in patients with Laron syndrome (primary GH insensitivity). *Eur J Endocrinol*. 2003;148(3):339-341.

12. Asa SL, Coschigano KT, Bellush L, Kopchick JJ, Ezzat S. Evidence for growth hormone (GH) autoregulation in pituitary somatotrophs in GH antagonist-transgenic mice and GH receptor-deficient mice. *Am J Pathol*. 2000;156(3):1009-1015.

13. Hofmann I et al. Linkage between growth retardation and pituitary cell morphology in a dystrophin-deficient pig model of Duchenne muscular dystrophy. *Growth Horm IGF Res*. 2020;51:6-16.

14. Albl B, Haesner S, Braun-Reichhart C, et al. Tissue sampling guides for porcine biomedical models. *Toxicol Pathol*. 2016;44:414-420.

15. Hofmann I, Kemter E, Fiedler S, et al. A new method for physical disector analyses of numbers and mean volumes of immunohistochemically labeled cells in paraffin sections. *J Neurosci Methods*. 2021;361: 109272.

16. Blutke A, Wanke R. Sampling strategies and processing of biobank tissue samples from porcine biomedical models. *JoVE*. 2018;133:e57276.

17. Stierhof Y-D, Hermann R, Humbel BM, Schwarz H. Use of TEM, SEM, and STEM in imaging 1-nm colloidal gold particles. In: Hayat MA, ed. *Immunogold-Silver Staining*. CRC Press; 1995:97-118.

18. Delesse M. Procédé mecanique pour determiner la composition des roches. *CR Acad Sci Paris*. 1847;25:544-545.

19. Howard V, Reed M. *Unbiased stereology: three-dimensional measurement in microscopy*. Garland Science; 2004.

20. Weibel E. Practical methods for biological morphometry. *London Stereol Methods*. 1979;1:40-116.

21. Blutke A, Schneider MR, Wolf E, Wanke R. Growth hormone (GH)-transgenic insulin-like growth factor 1 (IGF 1)-deficient mice allow dissociation of excess GH and IGF 1 effects on glomerular and tubular growth. *Physiol Rep*. 2016;4(5):e12709.

22. Tyanova S, Temu T, Cox J. The MaxQuant computational platform for mass spectrometry-based shotgun proteomics. *Nat Protoc*. 2016; 11(12):2301-2319.

23. Cox J et al. Andromeda: a peptide search engine integrated into the MaxQuant environment. *J Proteome Res*. 2011;10(4):1794-1805.

24. Cox J, Hein MY, Luber CA, Paron I, Nagaraj N, Mann M. Accurate proteome-wide label-free quantification by delayed normalization and maximal peptide ratio extraction, termed MaxLFQ. *Mol Cell Proteomics*. 2014;13(9):2513-2526.

25. Tyanova S, Temu T, Sinitcyn P, et al. The Perseus computational platform for comprehensive analysis of (prote)omics data. *Nat Methods*. 2016;13(9):731-740.

26. R Core Team (2021), *R: A Language and Environment for Statistical Computing*. R Foundation for Statistical Computing.

27. Tusher VG, Tibshirani R, Chu G. Significance analysis of microarrays applied to the ionizing radiation response. *Proc Natl Acad Sci U S A*. 2001;98(9):5116-5121.

28. Gu Z, Eils R, Schlesner M. Complex heatmaps reveal patterns and correlations in multidimensional genomic data. *Bioinformatics*. 2016; 32(18):2847-2849.

29. Liao Y, Wang J, Jaehnig EJ, Shi Z, Zhang B. WebGestalt 2019: gene set analysis toolkit with revamped UIs and APIs. *Nucl Acids Res*. 2019; 47(W1):W199-W205.

30. Perez-Riverol Y, Csordas A, Bai J, et al. The PRIDE database and related tools and resources in 2019: improving support for quantification data. *Nucl Acids Res*. 2019;47(D1):D442-d450.

31. Veldhuis JD, Keenan DM, Pincus SM. Motivations and methods for analyzing pulsatile hormone secretion. *Endocr Rev*. 2008;29(7): 823-864.

32. Laron Z, Kopchick JJ. *Laron Syndrome-from Man to Mouse*. Springer; 2011.

33. Tvilling L et al. Anatomy and histology of the Göttingen minipig adenohypophysis with special emphasis on the polypeptide hormones: GH, PRL, and ACTH. *Brain Struct Funct*. 2021;226:2375-2386.

34. Mitrofanova LB, Konovalov PV, Krylova JS, Polyakova VO, Kvetnoy IM. Plurihormonal cells of normal anterior pituitary: facts and conclusions. *Oncotarget*. 2017;8(17):29282-29299.

35. Kuwahara S, Sari DK, Tsukamoto Y, Tanaka S, Sasaki F. Age-related changes in growth hormone (GH) cells in the pituitary gland of male mice are mediated by GH-releasing hormone but not by somatostatin in the hypothalamus. *Brain Res*. 2004;998(2): 164-173.

36. Ariyasu D, Yoshida H, Hasegawa Y. Endoplasmic reticulum (ER) stress and endocrine disorders. *Int J Mol Sci*. 2017;18(2):382.

37. Bernard DJ, Brûlé E. Chapter 7 – anterior pituitary: glycoprotein hormones from Gonadotrope (FSH and LH) and Thyrotrope (TSH) cells. In: Litwack G, ed. *Hormonal Signaling in Biology and Medicine*. Academic Press; 2020:119-144.

38. Hauck SJ, Hunter WS, Danilovich N, Kopchick JJ, Bartke A. Reduced levels of thyroid hormones, insulin, and glucose, and lower body core temperature in the growth hormone receptor/binding protein knockout mouse. *Exp Biol Med*. 2001;226(6):552-558.

39. Sjogren K et al. Disproportional skeletal growth and markedly decreased bone mineral content in growth hormone receptor −/− mice. *Biochem Biophys Res Commun*. 2000;267(2):603-608.

40. Shea BT, Hammer RE, Brinster RL. Growth Allometry of the organs in giant transgenic mice*. *Endocrinology*. 1987;121(6):1924-1930.

41. Musumeci G, Castorina S, Castrogiovanni P, et al. A journey through the pituitary gland: development, structure and function, with emphasis on embryo-foetal and later development. *Acta Histochem*. 2015; 117(4–5):355-366.

SUPPORTING INFORMATION

Additional supporting information can be found online in the Supporting Information section at the end of this article.